Int. J. Electrochem. Sci., 17 **(2022)** Article Number: 220638, doi: 10.20964/2022.06.28

International Journal of
ELECTROCHEMICAL
SCIENCE
www.electrochemsci.org

Electrical Properties and Alkali-Pathways Simulation of New Mixed Ionic Conductor $Na_2K_2Co_{5.5}Al(AsO_4)_6$

Amira Marzouki[1,], Ameni Brahmia[2,3], Yara N. AlTherwah[2], Mutasem Z. Bani-Fwaz[2], Mohamed Hussien[2,4],Riadh Marzouki[2,5,**], Mohamed Faouzi Zid[6]*

[1] Laboratory of Signal Image and Energy Mastery, Engineering National Higher School of Tunis, Tunis, Tunisia
[2] Chemistry Department, College of Science, King Khalid University, Abha 61413, Saudi Arabia
[3] Laboratoire des Materiaux et de l'Environnement pour le Developpement Durable, LR18ES10, University of Tunis El Manar, 2092, Tunisia
[4] Pesticide Formulation Department, Central Agricultural Pesticide Laboratory, Agricultural Research Center, Dokki, Giza 12618, Egypt
[5] Chemistry Department, Faculty of Sciences of Sfax, University of Sfax, 3038, Tunisia
[6] Laboratory of Materials, Crystallochemistry and Applied Thermodynamics, Faculty of Sciences of Tunis, University of Tunis El Manar, Tunisia.
[*]E-mail : amira_marzouki@hotmail.com, rmarzouki@kku.edu.sa

Received: 1 March 2022 / *Accepted:* 7 April 2022 / *Published:* 7 May 2022

A new disodium dipotassium cobalt aluminate hexaarsenate $Na_2K_2Co_{5.5}Al(AsO_4)_6$ was synthesized by solid state route at 1193 K. The crystalline structure was determined by X-ray diffraction at room temperature. The new member of β-Xenophyllite material crystallizes in the monoclinic of the C2/m space group with the unit cell parameters: a=10.738(3) Å, b= 14.793 (2) Å, c=6.723(3) Å, β = 105.365° (10), V= 1336.8(4) $Å^3$ and Z=4. The crystal structure validation was carried out using Bond Charge distribution (CHARDI) and Bond Valence Sum (BVS) tools. The anionic framework can be described as tridimentionnal anionic framework sowing large hexagonal tunnels along [100] direction where the sodium and potassium cations are located. The electrical property of the title material was characterized by impedance spectroscopy technique from 553 to 753K temperature range using the frequency response analyzer with 0.05V amplitude signal over the range of 13MHz-5Hz. The conductivity value of the sample at 533K is 2.06×10^{-5} $S.cm^{-1}$, the activation energy Ea = 0.536eV, show that the $Na_2K_2Co_{5.5}Al(AsO_4)_6$ compound is an ionicconductor. The alkali ions conduction pathways in the studied compound were simulated via the bond valence site energy model (BVSE).

Keywords: X-ray diffraction, Alkai-based material, Electrical properties, Transport pathways simulation.

1. INTRODUCTION

The crystallographic systems *A*–Co/Al–P/As–O (*A*: monovalent cation) have shown a variety of structural types in recent years, including $LiCoXO_4$ (*X*=P, As) [1, 2], $Co_xAl_{1-x}PO_4(NH_4)_x(NH_3)_{0.5-x}$ (x 0.4) [3, 4], and $Na_{0.09}(Co_{0.06}Al_{0.96})$ (PO4) [4], $Ag_{3.39}Co_2(P_2O_7)_2$ [5], triclinic form pyrophosphate in the, $A_2CoP_2O_7$, displaying bidimensional framework as mellilite structure [6, 7], $ACo_3H_2(AsO_4)_3$ (*A*=Na, Ag) [8, 9] alluaudites-like arsenate and $Na_4Co_{5.63}Al_{0.91}(AsO_4)_6$ [10] as Xenophellite material. In this regard, we investigated the A_2O-CoO/Al_2O_3-X_2O_5 (*A* = monovalent cation, *X* = P or As) systems, which are still understudied. Solid state reaction was used to prepared the $Na_4Co_{5.63}Al_{0.91}(AsO_4)_6$ compound in single-crystal and polycrystalline forms [11]. The structural analysis revealed that in the arsenate materials the Na^+ cations in a three-dimensional structure with hexagonal canals. The study of structural properties paves the pathways for a better understanding of electrical properties. As a result, the structural data, open framework, partial occupations, and significant agitations of Na+ ions in big tunnels indicate that these features encouraged ionic mobility.

The goal of this study is to use XRD single crystal, XRD Powder, and EDX techniques to analyze the $Na_2K_2Co_{5.5}Al(AsO_4)_6$ material. The electrical investigation was carried out via impedance spectroscopy in order to optimize the sintering conditions and microstructure. The Bond Valence Site Energy BVSE model was used to investigate the relationship between structure and ionic conductivity.

2. EXPERIMENTAL AND COMPUTATIONAL METHODS

The title material was synthesized as single crystal and polycrystalline powder using the solid-state route. Commercial chemicals were obtained and employed without additional purification. Previous works provide more information on the synthesis procedure [12]. In this work, potassium and sodium was taken in an equivalent molar ratio Na:K = 1:1. The crystallinity of the sample was first verified under polarizing microscope then by using the single crystal diffractometer.

In a platinum crucible, a mixture of high-purity reagents ($NaNO_3$, KNO_3, $Co(NO_3)_2.6H_2O$, Al_2O_5, and As_2O_5) is mixed in the stoichiometric ratios of the single crystal $Na_2K_2Co_{5.5}Al(AsO_4)_6$. The sample is progressively annealed in air to 673K for 24 hours to eliminate volatile products. Pellets-shaped samples were generated in a second step by uniaxial pressing at 2kbar and heating at 1143 K for 3 days. The material was brought to room temperature gradually. The single-crystal structure was confirmed by the powder X-ray diffraction pattern.

For the single crystal structure determination, a suitable single crystal with dimensions of 0.27×0.24×0.1 mm3 was selected. The structural data was obtained using the MoK (=0.71073) radiation on an Enraf-Nonius CAD-4 [13-14] diffractometer at room temperature. The standard corrections were used, as well as absorption through a psi-scan [15] and secondary extinction correction [16] for Lorentz and polarization effects. The SHELX-97 [16] computer programs contained in the WinGX software package [17] were used for all subsequent computations. The Diamond 3 software [18] was used to view the crystal structure.

Charge Distribution analysis CHARDI [19–20] and Bond Valence Sum BVS [21-22] were performed with the CHARDI2015 [20] and SoftBV [23] programs as validation tools, respectively.

Energy-Dispersive X-ray Spectroscopy (EDX) and microstructure control was performed by SEM using an apparatus of the type Quanta 200.

At room temperature, an X-ray powder diffraction pattern was recorded using a Philips D8 diffractometer with copper anticathode K (=1.5406) covering the range of 10° to 70°, with a step of roughly 0.02°.

The measurements were preceded by a pretreatment of the samples in order to lower the mean particle size of the generated powder to control the relative density of the ceramic for the evaluation of the electrical properties, with the goal of obtaining dense ceramic. After that, the material was ball-milled in ethanol using a FRITSCH planetary micromill pulverisette device with agate jars and agate balls. A lesser amount of powder (5 g) and six agate balls (about 10 mm diameter) are placed in the agate jars for ball milling. To prevent pollutants and unnecessary heating during the experiment, the grinding was done in ethanol. For the course of the experiment, 10 minutes milling sessions were alternated with 5 minutes stop sequences. Despite the presence of ethanol, milling is still an intense operation that results in a significant heating of the entire apparatus. Between two milling operations, the pause phase allows the system to cool down.

Pellet samples of various relative densities were compacted using a uniaxial press, followed by a sintering in air at 1143 K for 2 hours (5 K.min-1 heating and cooling rates). Utilizing a Hewlett Packard 4192A with frequency response analyser (F.R.A.) in the 13x106 Hz – 5Hz frequency range, electrical measurements were recorded in air using complex impedance spectroscopy. R.F. magnetron sputtering was used to deposit silver electrodes on the two faces of each sample. The analysis was carried out at the open circuit voltage with a 50 mV supplied AC voltage. The sample was connected to the F.R.A. by platinum grids and wires, then placed in a Pyrox furnace in a stainless steel sample holder inside an alumina tube. The relative densities of the ceramic were calculated using precise measurements of sample sizes and weights, as well as a comparison to the theoretical density derived from the crystal structure.

The sodium migration in the interlayer space was simulated using the BVSE (Bond Valence Site Energy) model [22-23]. The BVSE model is a more recent evolution of Pauling's (1929) [24] BVS model for explaining the production of inorganic compounds. Brown & Altermatt 1985 [25] and Adams 2001 [23] enhanced the BVS model, resulting in the following formula for an individual bond-valence sA-X:

$$s_{A-X} = \exp\left(\frac{R_0 - R_{A-X}}{b}\right) \quad (1)$$

The distance between counter-ions A and X is given by RA-X, and R0 and b are fitted constants, with R0 being the length of a unit valence bond.

Since 1999, the BVS model is adopted in the anionic framework to simulate cation transportation by following the valence unit as a function of migration distance [26]. Adams proposed a method for relating valence units to potential energy scales that took electrostatic interactions into account in 2011. See the references [22-23] for further information on the model. The 3DBVSMAPPER algorithm was used to calculate the BVSE using Na+ as a test ion and default parameters [26].

3. RESULTS AND DISCUSSION

3.1. Crystal structure determination and validation

The structure resolution is carried out by direct methods using the SHELXS-97 software [16]. Three peaks attributed to cobalt atoms, one to aluminum, another to arsenic, and a few oxygen atoms are located first. The obtained results are refined by the SHELXL-97 software [16]. The unit cell parameters of the title material are very close to the arsenate $Na_4Co_{5.63}Al_{0.91}(AsO_4)_6$. The structure was therefore solved based on the atomic coordinates of this isotype material. In the first step, the coordinates and thermal agitation factors of the cobalt/aluminium, arsenic and oxygen atoms were resolved. At this stage, the reliability factors are R = 0.21 and Rw (F2) = 0.42. The feasibility factors R and Rw then converge towards 0.171 and 0.372, respectively. The high agitations of the Co/Al elements prompted us to an additional refinement of their occupations. The obtained occupation is five significant peaks appearing in the Fourier-Difference synthesis were observed near Na1, Na2 and Na3 cations. These peaks were attribute to the fraction of potassium ions. Three simultaneous constraints EXYZ, EADP and SUMP are used on the Na:K sites with 0.5:0.5 occupatins. The obtained agitations are satisfactory and the final refinement of the atomic parameters in anisotropic thermal agitation mode brought these factors down to R = 0.031 and Rw (F2) = 0.094 where the empirical formula is $Na_2K_2Co_{5.5}Al(AsO_4)_6$. A summary of the crystallographic data, conditions of the data collection and the structure refinement results is given in Table 1. The atomic coordinates and the equivalent isotropic thermal factors are in Table 2.

Table 1. Summary of crystallographic data of $Na_2K_2Co_{5.5}Al(AsO_4)_6$.

Crystal data	
Empirical formula	$Na_2K_2Co_{5.5}Al(AsO_4)_6$
Crystal system ; Space group	Monoclinic; C2/m
Unit cell parameters	a = 10.7381 (3) Å; b= 14.793 (3) c = 6.723 (3) Å β = 105.365 ° (10)
Volume ; *Z*	1033.2(4) $Å^3$; 2
Formula weight ; $\rho_{calc.}$	1336.88 $gmol^{-1}$; 4.311 gcm^{-3}
Absorption coefficient (μ)	14.571 mm^{-1}
Crystal sharp ; color	Parallelepiped ; pink
Crystal size	0.27 × 0.22 × 0.17 mm
Data collection	
Diffractometer	Enraf-Nonius CAD-4
Wavelength ; Temperature	$\lambda_{Mo\ K\alpha}$=0.71073 Å ; 298(2) K
Theta range for data collection	2.4° ≤θ ≤ 26.97°
Limiting indices	-13 ≤*h*≤ 13 ; -1≤*k*≤ 18 ; -8 ≤*l*≤ 1
Scan mode	ω/2θ
Absorption correction ; T_{min} ; T_{max}	psi-scan ; 0.076; 0.054
Standards; frequency (min); decay (%)	2 ; 120 ; 1
Reflections collected	1448

Refinement	
Refinement method	Full-matrix least-squares on F^2
Final R indices [$I > 2\sigma(I)$]	R(F)= 0.031; wR(F^2)= 0.094,
Reflections ; parameters	1146; 116
$\Delta\rho_{max}$; $\Delta\rho_{min}$ ($eÅ^{-3}$)	0.80 ; -0.77
Goodness of fit (S)	1.103

Table 2. Atomic coordinates and equivalent isotropic thermal factors in $Na_2K_2Co_{5.5}Al(AsO_4)_6$.

Atom	**x**	**y**	**z**	**U_{eq}^*(Å^2)**	**Occ. (<1)**
As1	0.598149 (5)	0.320868 (7)	0.289009 (5)	0.00696 (7)	
As2	0.821023 (3)	½	0.061819 (7)	0.00755 (10)	
Co1	0.320159 (5)	0.318455 (7)	0.180649 (3)	0.00811 (8)	0,286 (11)
Al1	0.320159 (5)	0.318455 (7)	0.180649 (3)	0.00811 (8)	0,714 (11)
Co2	0	0.664005 (7)	0	0.01241 (6)	0,607 (8)
Al2	0	0.664005 (7)	0	0.01241 (6)	0,143 (8)
Co3	½	½	0	0.00687 (8)	
O1	0.991924 (3)	0.266416 (3)	0.271529 (5)	0.01132 (6)	
O2	0.690654 (5)	0.291436 (7)	0.130191 (3)	0.01661 (8)	
O3	0.939341 (5)	½	0.277716 (5)	0.01607 (7)	
O4	0.831376 (3)	0.591728 (3)	-0.086272 (4)	0.02120 (9)	
O5	0.690296 (5)	0.349081 (7)	0.522433 (5)	0.01229 (6)	
O6	0.680672 (4)	½	0.126304 (5)	0.01064 (11)	
O7	0.487546 (7)	0.406127 (3)	0.202779 (5)	0.00942 (7)	
Na1	0.073380 (5)	0.115487 (3)	0.492822 (8)	0.02991 (11)	0..25
K1	0.073380 (5)	0.115487 (3)	0.492822 (8)	0.02991 (11)	0.25
Na2	0. 682812 (5)	½	0.423131 (9)	0.03732 (12)	0.25
K2	0.682812 (5)	½	0.423131 (9)	0.03732 (12)	0.25
Na3	0.928771 (9)	½	0.476221 (9)	0.06394 (8)	0.25
K3	0.928771 (9)	½	0.476221 (9)	0.06394 (8)	0.25
$^{(*)}Uéq = (1/3)\sum_i\sum_j U^{ij}a_i^*a_j^*a_i.a_j$					

Bond valence sum model BVS [21-22] and charge distribution method CHARDI [23-24] validation tools supported the proposed structural model. The formal oxidation numbers agree with the valence sums, V, calculated using the BVS model, and charges Q calculated using the CHARDI analysis. Table 4 summarises the results of the CHARDI and BVS calculations.

Table 4. CHARDI and BVS analysis of cation polyhedra in $Na_2K_2Co_{5.5}Al(AsO_4)_6$

Cation	q(i).sof(i)	Q(i)	V(i)	CN(i)	ECoN(i)
*M*1	2,714	2,810	2,701	6	5,912
*M*2	1,647	1,567	1,020	4	3,978
Co3	2,00	1,990	1,981	6	5,898
As1	5,00	5,033	5,011	4	3,990

As2	5,00	5,001	4,870	4	3,983
Na1/K1	0,50	0,498	0,471	5	4,589
Na2/K1	0,50	0,501	0,413	7	6,437
Na3/K1	0,50	0,504	0,471	6	5,970

*M*1=$Co_{0,286}Al_{0,714}$; *M*2=$Co_{0,607}Al_{0,143}\square_{0,250}$; q(i) : oxidation number;
sof(i) : taux d'occupation du site ; sodium CNs pour $d(Na–O)^{max}$=3,00 Å ;
$\sigma=[\Sigma_i(q_i-Q_i)^2/N-1]^{1/2}$=0,049.

Qualitative EDX analysis of the single crystal of $Na_2K_2Co_{5.5}Al(AsO_4)_6$ confirmed the existence of Co, As, Al, Na, K, and oxygen, confirming the presence of the previous elements. The sample holder produced a carbon peak (Figure 3).

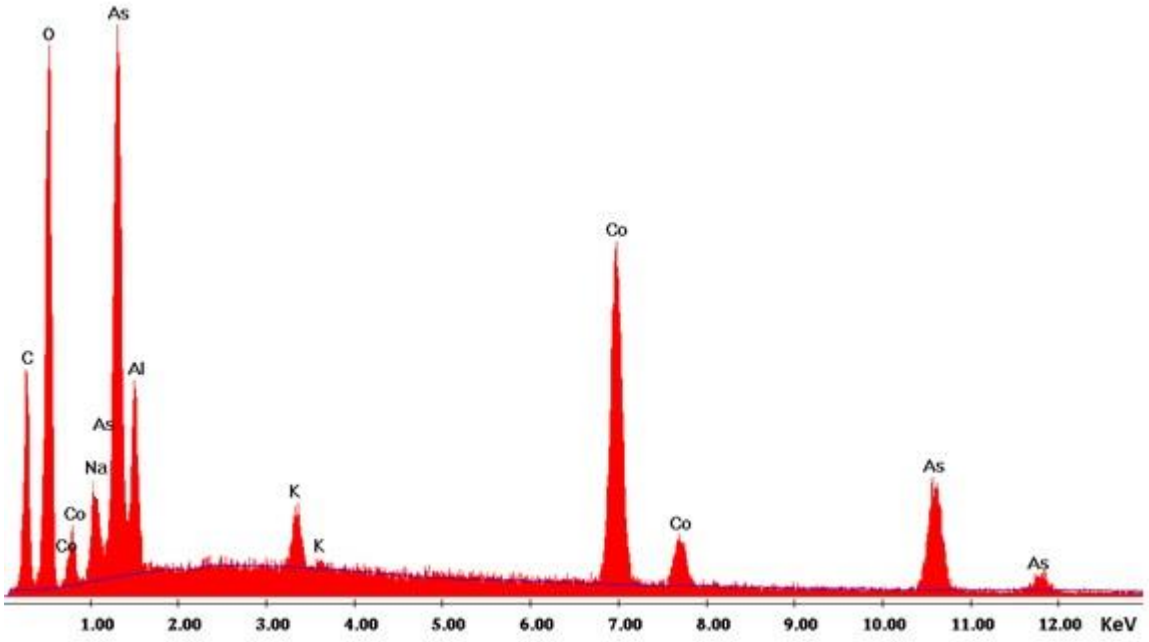

Figure 1. EDX spectrum of $Na_2K_2Co_{5.5}Al(AsO_4)_6$.

3.1. Crystal structure description

The $Na_2K_2Co_{5.5}Al(AsO_4)_6$ material is a new member of the $Ag_4Co_7(AsO_4)_6$ [27], $Na_4Co_7(AsO_4)_6$ [28], and $Na_4Co_{5.63}Al_{0.91}(AsO_4)_6$ [29] isostructural phases. Two tetrahedra AsO_4, two octahedra $Co3O_6$, and $M1O_6$ ($M1$ = $Co_{0.286}Al_{0.714}$) and $M2O_4$ ($M2$= $Co_{0.607}Al_{0.143}$) tetrahedra constitute the $Na_2K_2Co_{5.5}Al(AsO_4)_6$ structure. The polyhedra (Co, Al) are organized in the ab plan. The corners of the Co_2O_{10} octahedral units are joined by $M2O_4$ tetrahedra. Polyhedral chains propagate in the [100] direction as a result. The ribbons are connected by $M1O_6$ octahedra, while the windows in these plans are occupied by $As1O_4$ tetrahedra. $As2O_4$ tetrahedra share corners and edges with $M1O_6$ polyhedra, ensuring a connection between the plans. Hexagonal tunnels along a (Figure 4) connect with quadrilateral windows parallel to the [010] direction in the three-dimensional framework. The $(Na/K)^+$

cations spread on three distinct sites partially occupied at 50% are used to locate the tunnels. The agitation of the alkali cations is relatively high.

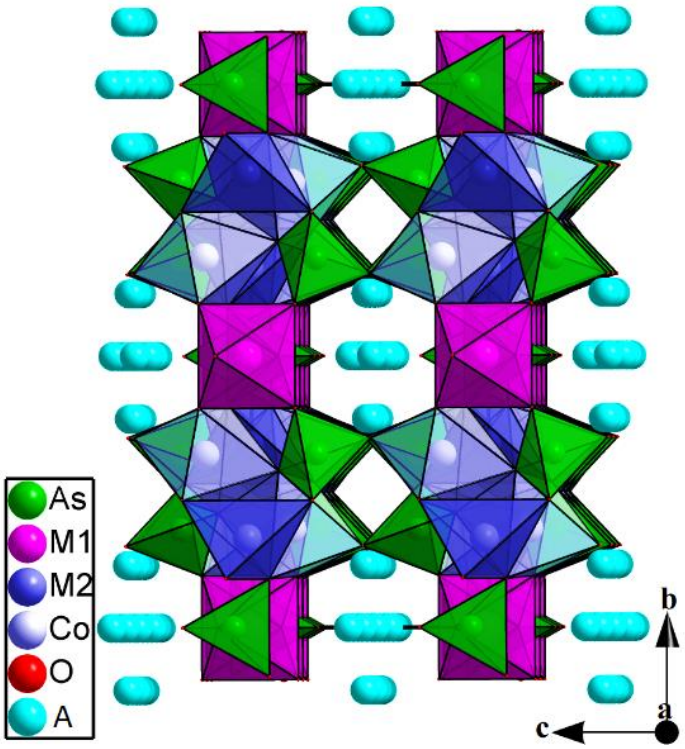

Figure 2. Projection of $Na_2K_2Co_{5.5}Al(AsO_4)_6$ structure along *a* direction

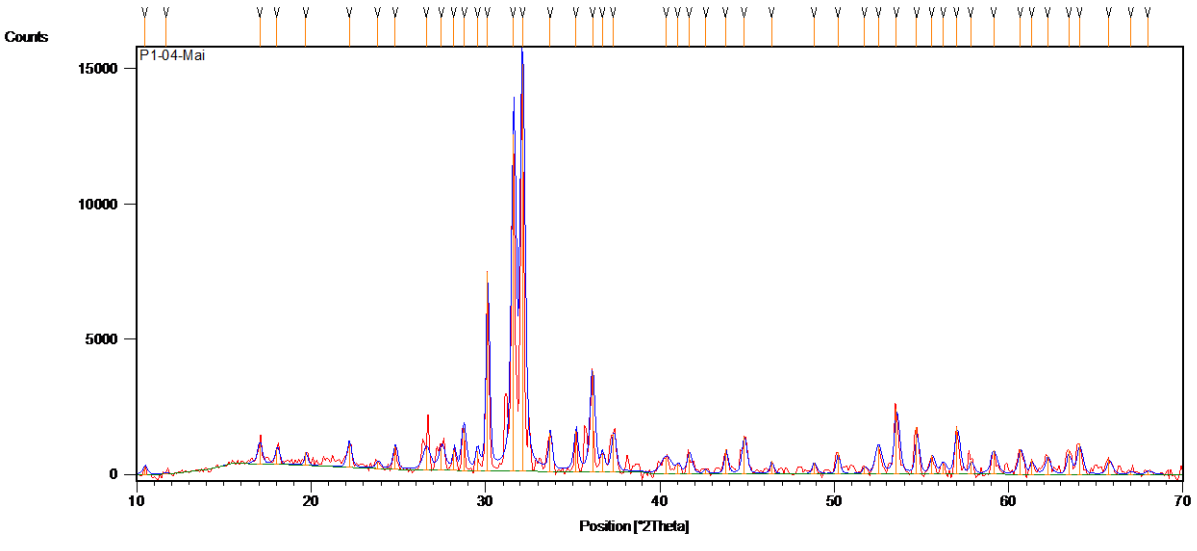

Figure 3. XRD pattern of the prepared powder of $Na_2K_2Co_{5.5}Al(AsO_4)_6$.

The anionic framework of the studied material is thus open, and alkali cation mobility through the tunnels appears to be possible, prompting us to investigate the ionic conduction of the studied material.

A Bruker D8 diffractometer was used to record an X-ray powder diffraction pattern using Cu anticathode K (=1.5406), in the from 10° to 70° with step of 0.02°, at room temperature. The XRD of the prepared powder and the XRD monocrystal determined from the crystallographic information file (CIF) of the single crystal are similar which confirm the purity of our material. The unit cell parameters of the prepared powder were determine using profile matching refinement via the X'Pert HighScore Software [30]: a = 10.736 (7) Å; b= 14.794 (8) c = 6.722 (7) Å and β = 105.36 ° (6) of the monoclinic system of the C2/m space group.

3.2. Infrared spectroscopy

Figure 5 shows the infrared spectrum measured in the region where the main vibrations occur.

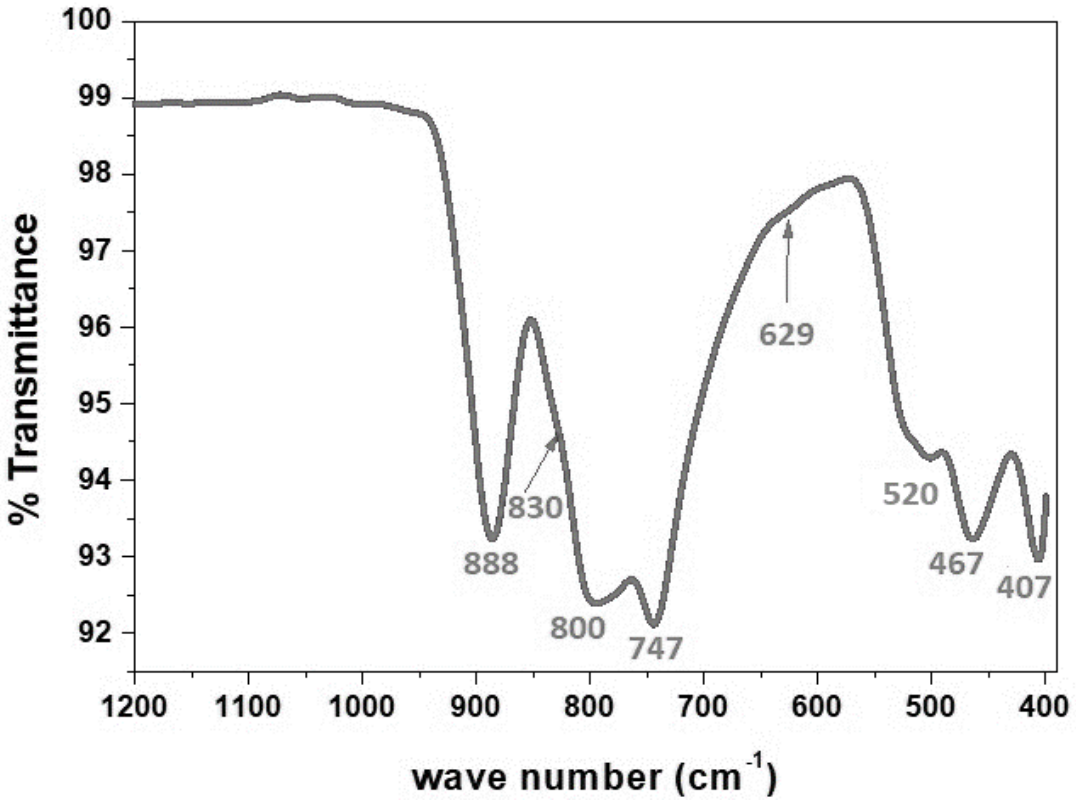

Figure 4. IR spectrum of $Na_2K_2Co_{5.5}Al(AsO_4)_6$ compound

Table 3 shows the vibrational bands assigned to the MO_4, AsO_4, and MO_6 groups, based on earlier work, particularly [11,29].

Table 3. Assignment of vibration frequencies in $Na_2K_2Co_{5.5}Al(AsO_4)_6$ compound *M*=(Co,Al)

Wave number (cm^{-1})	**Assignment**	**Wave number (cm^{-1})**	**Assignment**
407	$\nu_2(AsO_4)$	**747**	$\nu_1(MO_6)$
467	$\nu_4(AsO_4)$	**800**	$\nu_1(MO_4)$
520	$\nu_2(MO_6)$	**830**	$\nu_1(AsO_4)$
629	$\nu_3(MO_6)$	**888**	$\nu_3(AsO_4)$

3.3. Electrical properties

The measurements for the electrical analyses were preceded by a sample pretreatment to minimize the mean particle size of the acquired powder. Planatary grinding was carried out using FRISCH micromill pulverisette 7. Uniaxial pressing was followed by isostatic pressing at 2.5 kbar and sintering for 2 hours at 600 °C with 5 °C.min-1 heating and cooling rates. With a final diameter of 8 mm and a thickness of 2 mm, the sample obtained exactly 85% of the theoretical density after these treatments. To maintain good electric connections, platinum electrodes were glued to the two faces of the pellet with platinum paste. A Hewlett-Packard 4192a Impedance Analyzer was used to perform impedance spectroscopy studies. The impedance spectra were measured across a frequency range of 5 Hz to 13 MHz.

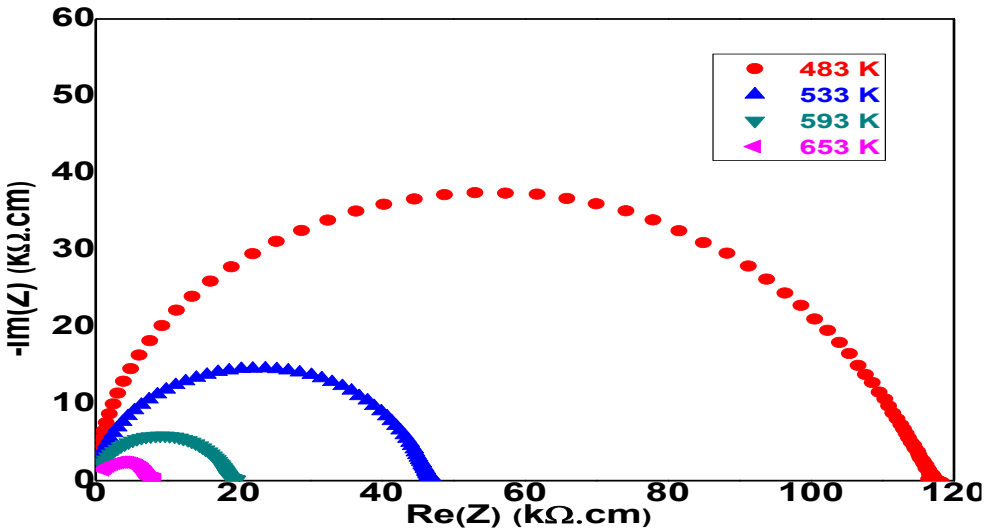

Figure 5. Impedance spectra of $Na_2K_2Co_{5.5}Al(AsO_4)_6$ recorded at 483-653K in air.

Complex impedance spectroscopy was used to determine the electrical characteristics of the title chemical. The electrical parameters were measured in air in the temperature range of 443–733 K after each phase of stabilization and in the frequency range of 5Hz–13MHz. The applied voltage was 0.5 V, which allowed aberrant points at low frequencies to be eliminated. The electrical parameters were determined using the Zview computer application [31] and a conventional electrical circuit as follows: CPE is a constant phase element in R/CPE-R/CPE:

$$Z_{CPE} = \frac{1}{A(j\omega)^p} \quad (4)$$

To account for instrumental contributions, especially at high temperatures, a supplemental inductance L was imposed. According to the following relationships, the true capacitance was determined from the pseudo-capacitance:

$$\omega_0 = (RA)^{-1/p} = (RC)^{-1} \quad (5)$$

where ω_0 = relaxation frequency, A = pseudo-capacitance calculated from the CPE, and C = the actual capacitance. Table 5 summarizes the electrical parameters.

Table 5. Electrical parameters of $Na_2K_2Co_{5.5}Al(AsO_4)_6$ determined by impedance spectroscopy

T (°C)	T (K)	1000/T (K^{-1})	Rt (10^4 Ω)	σ (10^{-5} S cm^{-1})	Ln(σ×T)
160	433	2.30946882	25.86	0.23	-7.66190007
210	483	2.07039337	7.06	0.86	-5.48901724
260	533	1.87617261	2.93	2.06	-4.51163079
320	593	1.68634064	1.18	5.10	-3.49778949
380	653	1.53139357	4.75	12.7	-2.48811313
445	718	1.39275766	1.90	31.9	-1.4753481
500	773	1.29366106	8.80	68.6	-0.63448641

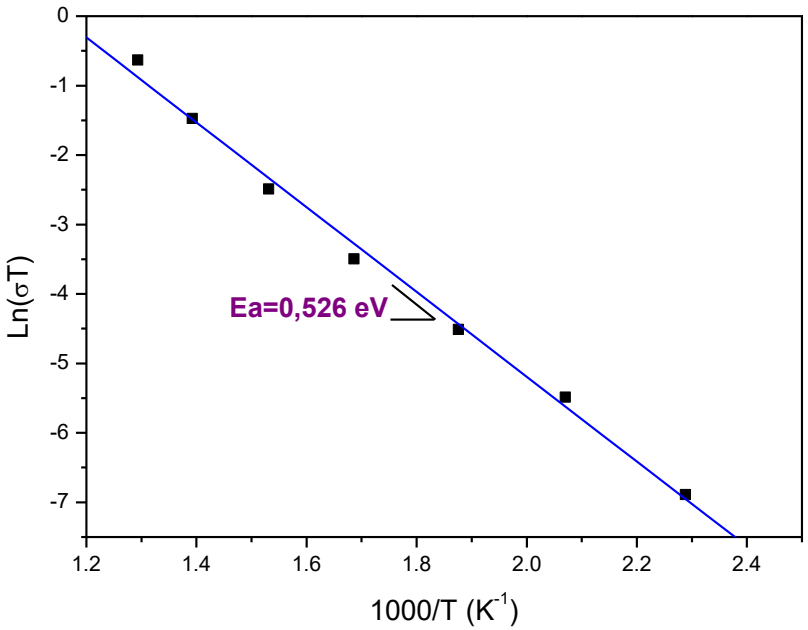

Figure 6. Arrhenius plot of conductivity of $Na_2K_2Co_{5.5}Al(AsO_4)_6$ sample.

The conductivity increases from 0.23× 10^{-5} S cm^{-1} at 160°C to 68.6 10^{-5} S cm^{-1} at 500 °C (Table 5). Although, the conductivity value of the title material at 320 °C is higher than that of the parent material $Na_4Co_7(AsO_4)_6$ (2.51× 10^{-5} S cm^{-1} at 360 °C [28]). The more critical parameter, the activation energy, decreases for $Na_4Co_7(AsO_4)_6$ compared to that of $Na_2K_2Co_{5.5}Al(AsO_4)_6$, i.e. 1.0 eV and 0.526 eV, respectively (Figure 6), in good agreement with the BVSE results discussed below.

3.4. Na^+ Transport pathways simulation

The BVSE simulation model was used to define the alkali-ion transport pathways in the anionic frameworks of the $Na_2K_2Co_{5.5}Al(AsO_4)_6$ via the 3DBVSMAPPER computer program.

Investigation of isosurfaces connecting sodium ion sites in the unit cells of isostructural materials show that the sodium can move along the *a* direction and form monodimensional infinite pathways (Fig. 7) while the calculated activation energy is 0.58 eV; suggest high ionic conductivity of the title material.

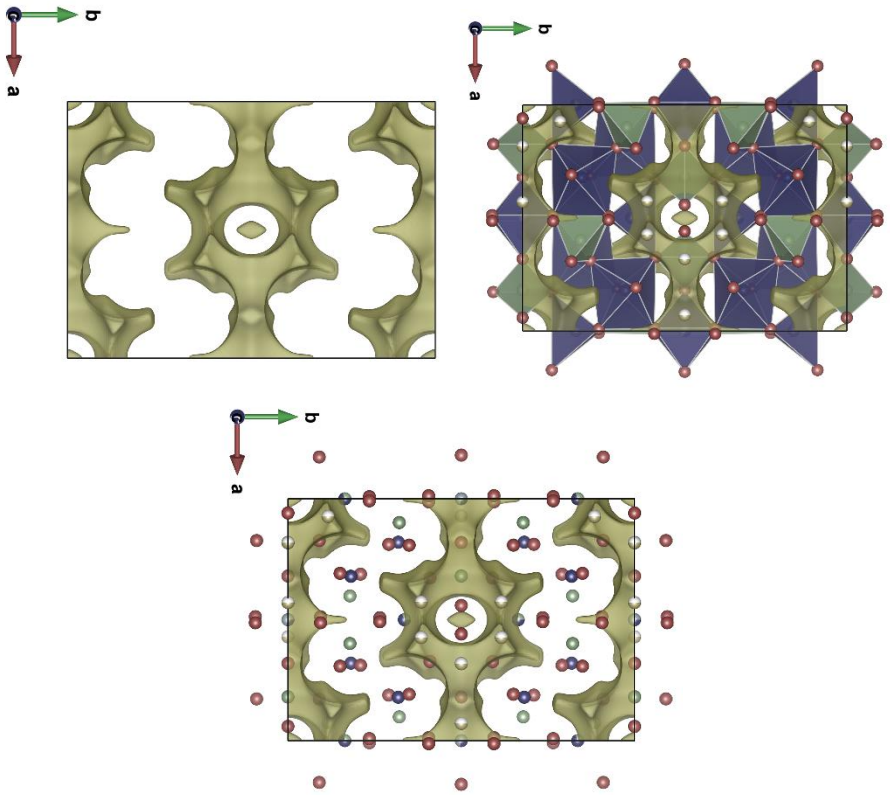

Figure 7. Projection along *c* direction of the $Na_2K_2Co_{5.5}Al(AsO_4)_6$ unit cell with coordination polyhera and without coordination polyhedra.

The BVS analyses support the structural studieswhich the most probable conduction pathways of the studied material are the tunnels of the *a* direction . Figure 8a shows the size of the hexagonal sections of tunnels . Two CoO_6 and two MO_6 octahedra, and two AsO_4 tetrahedra border these canals. These sections are the widest and therefore more conducive to sodium cation transport.

The [010] direction tends to be less favorable than the *a* direction. In fact, the square bases windows (Fig. 8b) produced along b direction have smaller section sized than those of the [100] direction, indicating that sodium ion migration is more advantageous in the *a* direction.

Crystallographic investigations, on the other hand, reveal that Co/Al substitution increase the tunnel section dimensions and also the unit cell parameters. In fact, the volume of the unit cell increase from V=1019.65(16) $Å^3$ in $Na_4Co_7(AsO_4)_6$ to V=1033.3(4) $Å^3$ in $Na_2K_2Co_{5.5}Al(AsO_4)_6$ which explain that the activation energy values of $Na_2K_2Co_{5.5}Al(AsO_4)_6$ are lower than that of $Na_4Co_7(AsO_4)_6$. In fact, sections tunnels along *a* direction in $Na_2K_2Co_{5.5}Al(AsO_4)_6$ are in the order: 4.467 - 4.823 Å. The tunnel sections along [100] direction $Na_4Co_7(AsO_4)_6$ are 4.636-4.730 Å.

Compared to activation energies of other phosphates such as $Na_{1.14}K_{0.86}CoP_2O_7$ (Ea = 1.34 eV) [32], $Na_{1.42}Ag_{0.58}CoP_2O_7$ (Ea = 1.37 eV) [33] and $Ag_{3.68}Co_2(P_2O_7)_2$ (Ea = 1.7 eV) [5] and other sodium compounds such as $Na_4Co_{5.63}Al_{0.91}(AsO_4)_6$ (Ea = 0.53 eV) [11] and sodium-cellulose (Ea = 0.49 eV and 0.68 eV) [34], $Na_2K_2Co_{5.5}Al(AsO_4)_6$ exhibit high electric conductivity with an activation energy value of 0.536 eV.

4. CONCLUSION

The studied compound, has been synthesized by solid-state reaction. Its structure has been determined by single-crystal XRD. FTIR spectroscopy show the existence of the vibrational group of the MO_6 and MO_4 (M=Co/Al) polyhedra. The Bond valence sum model (BVS) and charge distribution method (CHARDI) were used to approve the structural model. This structure, isostructural to $Na_2K_2Co_{5.5}Al(AsO_4)_6$, shows an open anionic framework facilitating monodimensional Na ionic conductivity. The modification of the crystallographic datadue to the Al/Co substitution reduces the activation energy of Na conductivity, as confirmed by impedance spectroscopy measurements and supported by BVSE simulation. Overall, our study suggests that the Al/Co substitution in the $Na_2K_2Co_{5.5}Al(AsO_4)_6$, can further improve Na ionic conductivity and thus rate capability of $Na_2K_2Co_{5.5}Al(AsO_4)_6$, based cathodes.

ACKNOWLEDGMENT
The authors extend their appreciation to the Deanship of Scientific Research at King Khalid University for funding this work through research groups program under grant number GRP-272-42.

References

1. F. Erragh, A. Boukhari and E. M. Holt, *Acta Crystallogr. C Struct. Chem.*, 52 (8) (1996) 1867
2. M. V. V. M. Satya Kishore and U. V. Varadaraju, *Mater. Res. Bull.*, 41 (3) (2006), 601
3. P. B. Ranko and C. S. Slavi, *J. Mater. Chem.*, 9 (1999) 2679
4. G. Muncaster, G. Sankar, C. R. A. Catlow, J. M. Thomas, R. G. Bell, P. A. Wright, S. Coles, S. J. Teat, W. Clegg and W. Reeve, *Chem. Mater.*,11 (1999)158
5. M. A. Ben Moussa, R. Marzouki, A. Brahmia, S. Georges, S. Obbade and M. F. Zid, *Int. J. Electrochem. Sci.*, 14 (2019) 1500

6. P. Barpanda, M. Avdeev, C. D. Ling, J. Lu and A. Yamada, Physical Inorganic Chemistry, 44(12) (2013) https://doi.org/10.1002/chin.201312005
7. F. Erragh, A. Boukhari, B. Elouadi and E. M. Holt, Journal of Crystallographic and Spectroscopic Research, 21(3) (1991)321
8. P. Keller, H. Riffel, F. Zettler and H. Hess, Z. *Anorg. Allg. Chem*., 474(3) (1981)123
9. K. Lii and P. Shih, *Inorg. Chem*. 33(14) (1994)3028
10. R. Marzouki, A. Guesmi and A. Driss, *Acta Crystallogr. C Struct. Chem*., 66 (2010)i95-98
11. R. Marzouki, A. Guesmi, M. F. Zid and A. Driss, Ann. *Chim. - Sci. Mat*., 38 (3-4) (2013) 117.
12. R. Marzouki, *Mater. Res. Express*, 7(1) (2020) 016313
13. A. J. M. Duisenberg, *J. Appl. Crystallogr*. 25 (1992) 92
14. J. Macíček and A. Yordanov, *J. Appl. Crystallogr*., 25 (1992) 73-80
15. A. C. T. North, D. C. Phillips and F. S. Mathews, *Acta Crystallogr*., A 24 (1968) 35116 G. M. Sheldrick, *Acta Cryst*., C71 (2015) 3
16. G. M. Sheldrick, *Acta Cryst*. C71 (2015**)** 3-8. Doi: 10.1107/S2053273314026370
17. L. J. Farrugia, *J. Appl. Crystallogr*., 32 (1999) 837
18. K. Brandenburg, M. Berndt, Diamond Version 3. Crystal Impact. Bonn, 2001.
19. J.-G. Eon and M. Nespolo, *Acta Cryst*., B71 (2015) 34
20. M. Nespolo and B. Guillot, *J. Appl. Cryst*., 49 (2016) 317
21. S. Adams, *Acta Cryst*., B57 (2001) 278
22. I. D. Brown, The Chemical Bond in Inorganic Chemistry – The Bond Valence Model. IUCr Monographs on Crystallography, No. 12. Oxford University Press, 2002.
23. S. Adams, softBV. University of Gottingen, Germany, 2003. http://www.softbv.net.
24. L. Pauling, *J. Am. Chem. Soc*., 51 (1929) 1010
25. I. D. Brown and D. Altermatt, *Acta Cryst*., B41 (1985) 244
26. D. Mazza, *J. Solid State Chem*., 156 (2001) 154
27. R. Marzouki, A. Guesmi, S. Georges, M. F. Zid and A. Driss, *J. Alloy. Compd*., 586 (2014) 74
28. Y. Ben Smida, R. Marzouki, S. Georges, R. Kutteh, M. Avdeev, A. Guesmi and M.F. Zid, *J. Solid State Chem.,* 239 (2016) 8
29. Kazuo Nakamoto, Infrared and Raman Spectra of Inorganic and Coordination Compounds: Part A: Theory and Applications in Inorganic Chemistry, Sixth Edition, 2008 https://doi.org/10.1002/9780470405840.ch2
30. X'Pert HighScore Plus, PaNalytical B.V. Amelo, The Netherlands 2003.
31. D. Johnson, Zview version3.1c, Scribner Associates, Inc.,1990–2007.
32. R. Marzouki, Y. Ben Smida, A. Guesmi, S. Georges, I. H. Ali, S. Adams and M. F. Zid, *Int. J. Electrochem. Sci.,* 13 (2018) 11648
33. R. Marzouki, A. Guesmi, M. F. Zid and A. Driss, Crystal Structure Theory and Applications, 1 (2013) 68
34. R. Marzouki, A. Brahmia, S. Bondock, S. M. A. S. Keshk, M. F. Zid, A. G. Al-Sehemi, A. Koschella and T. Heinze, *Carbohydr. Polym*. 221 (2019) 29